

Article citation info:

Pawelski Z, Uszpolewicz G, Zdziennicki Z. Testing capabilities of a new test rig, with a planetary gear unit examined as an example. The Archives of Automotive Engineering – Archiwum Motoryzacji. 2017; 77(3): 111-132, <http://dx.doi.org/10.14669.VOL.77.ART8>

ATESTING CAPABILITIES OF A NEW TEST RIG, WITH A PLANETARY GEAR UNIT EXAMINED AS AN EXAMPLE

MOŻLIWOŚCI BADAWCZE NOWEGO STANOWISKA NA PRZYKŁADZIE PRZEKŁADNI PLANETARNEJ

ZBIGNIEW PAWELSKI, GRZEGORZ USZPOLEWICZ, ZBIGNIEW ZDZIENNICKI

Lodz University of Technology (TUL)¹

Summary

The article describes a test rig built at the Department of Vehicles and Fundamentals of Machine Design, Lodz University of Technology (TUL), for static and dynamic examination of vehicle and machinery driveline components. Adequate installed power of the propulsion system and extensive instrumentation of the test rig makes it possible to examine various prototype mechanical transmission units with power capacities of up to several ten kilowatts and to carry out a broad spectrum of measurements with high accuracy. During the tests, such variables as vibrations in any direction, gear shaft speeds, torques, noise levels, and various oil parameters, e.g. temperature, moisture content, or ferromagnetic debris content, may be recorded. Additional equipment enables precise alignment of all the rotating parts in the test rig drive train and determination of oil viscosity before and after the test. An important feature of the test rig is a possibility of changing the drive direction without demounting the object under test. This can be done thanks to an inverter control system, which enables electric machine operation modes to be switched over from motor to generator and vice versa. In the subsequent part of the article, selected results of testing a planetary gear unit with a geometric gear ratio of 3.1372 have been presented, which include efficiency, FFT

¹ Lodz University of Technology, Department of Vehicles and Fundamentals of Machine Design, ul. Żeromskiego 116, 90-924 Łódź, Poland,
e-mail:zbigniew.pawelski@p.lodz.pl
e-mail:grzegorz.uszpolewicz@p.lodz.pl
e-mail:zbigniew.zdziennicki@p.lodz.pl

analysis of vibrations, and noise level data. The test results have confirmed the suitability of the test rig for multipurpose applications and for comprehensive diagnosing of driveline components.

Keywords: power-circulating test rig, planetary gear unit, mesh and signature frequencies, vibrations and their FFT analysis, kinematic and dynamic gear ratio, noise level, efficiency measurements, efficiency adjusted to a uniform oil temperature

Streszczenie

W artykule opisano stanowisko do statycznych i dynamicznych badań podzespołów układów napędowych zbudowane w Katedrze Pojazdów i Podstaw Budowy Maszyn Politechniki Łódzkiej. Moc urządzeń napędowych zainstalowana na stanowisku, pozwala na badanie różnych prototypów przekładni mechanicznych o mocach do kilkudziesięciu kilowatów a bogate jego oprzyrządowanie umożliwia przeprowadzenie szerokiego spektrum pomiarów z wysoką dokładnością. W trakcie badań rejestrowane są takie zmienne jak drgania w dowolnym kierunku, prędkości obrotowe wałów przekładni, momenty obrotowe, poziom hałasu oraz parametry oleju takie jak temperatura, zawartość wilgoci i ścieru ferromagnetycznego. Dodatkowe wyposażenie umożliwia precyzyjne ustawienie współosiowe wszystkich elementów wirujących w linii napędowej stanowiska oraz określenie lepkości oleju przed i po badaniach. Istotną cechą stanowiska jest możliwość zamiany kierunku napędu bez demontażu badanego obiektu, co jest możliwe dzięki układowi sterowania falownikami umożliwiającemu zmianę charakteru pracy maszyn elektrycznych z silnika na generator i odwrotnie. W dalszej części przedstawiono wybrane wyniki badań przekładni planetarnej o przełożeniu kinematycznym 3,1372: określenie sprawności, analizę częstotliwościową drgań oraz poziom hałasu. Badania potwierdziły uniwersalność stanowiska i możliwość wszechstronnego diagnozowania podzespołów układów napędowych.

Słowa kluczowe: stanowisko z mocą krążącą, przekładnia planetarna, częstotliwości charakterystyczne i ząbienia, drgania i analiza fft, przełożenie kinematyczne i dynamiczne, poziom hałasu, pomiary sprawności, sprawność korygowana do określonej temperatury oleju

1. Introduction

Planetary gears find wide application in various branches of industry. There is also extensive literature dedicated to the problems related to such gears. In an overwhelming majority, however, such publications deal with theoretical studies. The works that include experimental research are quite rare and the experiment results presented in such reports are only used to verify the results obtained from theoretical analyses. In consequence, the test rigs used for experimental works are designed for low power capacities and limited spectrum of measurement capabilities. The experimental tests that were carried out at various research centres covered the following issues: dynamic behaviour of planetary gearsets [2, 6] and the impact of load on the values of natural frequencies of such gears [2], analysis of sidebands at mesh frequencies [3, 8], impact of load torque on changes in the mesh frequencies [11, 13], vibrations and noise of gearsets [5, 7, 9], and diagnostics of planetary gear units [9, 10].

Fig. 1 shows a multipurpose test rig built at the Department of Vehicles and Fundamentals of Machine Design, Lodz University of Technology (TUL), for static and dynamic examination

of vehicle and machinery driveline components, whether with constant or variable gear ratio. Adequate installed power of the test rig propulsion system makes it possible to examine various prototype mechanical transmission units with power capacities of up to several ten kilowatts, designed for various industrial applications. Thanks to extensive instrumentation of the test rig and a very high accuracy class of the sensors provided (e.g. the accuracy of the HBM torque meters used is 0.01 %), a broad spectrum of very precise measurements may be carried out.



Fig. 1. Rig for the testing of driveline components. Object under test: a planetary gear unit.

1 – motor; 2 – generator; 3 – gear unit under test; 4 – oil cooling system;
5 and 6 – HBM torque meters (to measure the torque and rotational speed);
7 – vibration sensors; 8 – PT 100 sensor (invisible); 9 – microphone (invisible)

The test rig equipment consists of the following:

1. Two electric machines of 200 kW capacity, capable of operating in both the motor and generator mode. A common DC voltage bus makes it possible to transmit electric energy from the generator to the motor. Thus, only the energy necessary to make up power losses, equal to a small fraction of the energy circulating in the working drive train, is drawn from an external electric network. At the TUL Department mentioned above, such a concept of test rigs has been adopted since 1995 [3].
2. Two ABB frequency converters, whose power supply section is provided with a bridge rectifier and an input filter to reduce the harmonic interference coming from the external electric network.
3. Programmable controller, making it possible to plan and perform individual experiments (Fig. 2). Changes in the working parameters of the electric machines may follow rectangular, trapezoidal, and sinusoidal signals or sums of such signals; they

are limited by electrical characteristics of the frequency converters and windings of machines 1 and 2.

4. HBM data recorder to record and archive the data obtained from the test rig (Fig. 3). This apparatus functions separately from the programmable controller (Fig. 2) to prevent mutual interference between system components and to improve system operation safety. The measurement data are handled with the use of the HBM Catman Easy V3.5.1 software.
5. GTG AC102-1A sensors to measure gear housing vibrations in three directions, i.e. horizontal, vertical, and axial.
6. Prüftechnik SHAFTALIGN laser system (Fig. 4) for the aligning of shafts of all the units under test, clutches, and shafts in the test rig drive train to minimize the vibrations caused by shaft misalignment. The achieving of the required accuracy of alignment of all the joints cooperating in the test rig system is prerequisite for starting any test cycle (Fig. 2).
7. Lubricating and oil cooling system (item 4 in Fig. 1), adapted for the unit under test. In the drain line of the unit, wear debris sensor Kittiwake FG-K16583-KW, moisture-in-oil sensor Kittiwake FG-K16947-KW, and temperature sensor PT100 are installed. Additionally, the pre- and post-test oil viscosity is checked at an auxiliary test station (Fig. 5).

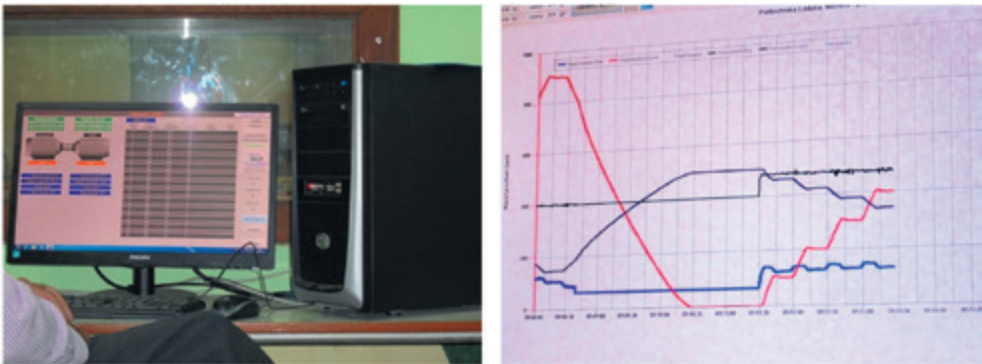


Fig. 2. Experiment planning and monitoring station: online digital and graphical monitoring of the parameters of operation of the electric machines

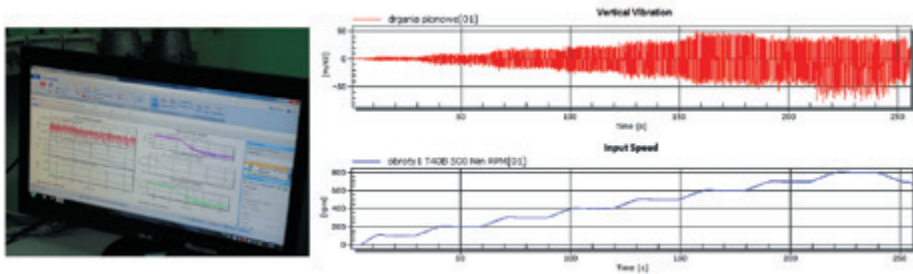


Fig. 3. Measuring data recording, archiving, and online monitoring station

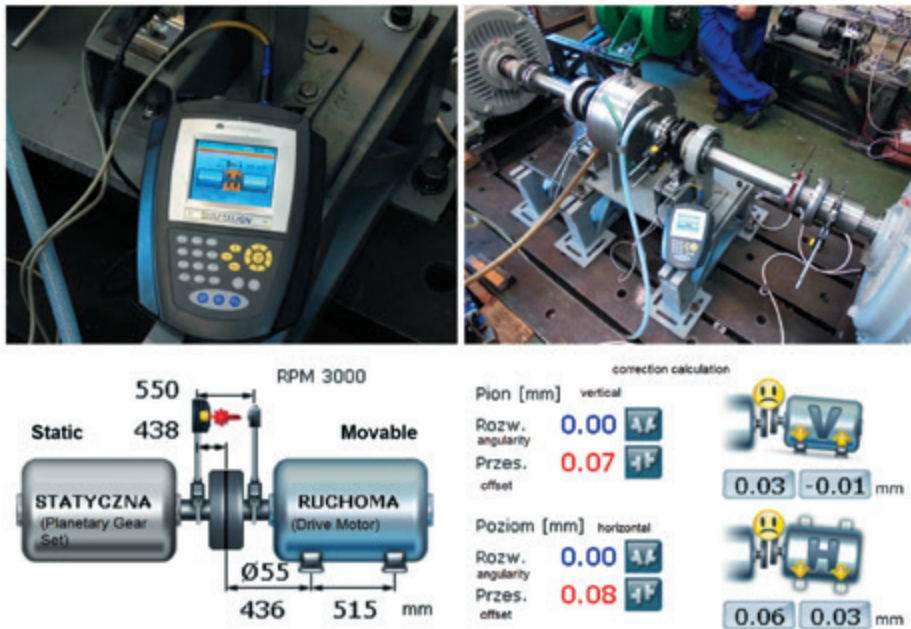


Fig. 4. Prüftechnik SHAFTALIGN laser system

With a temperature growth from 30 °C to 100 °C, the oil viscosity may drop to as low a value as one tenth of the initial level (Fig. 5), with the smallest changes occurring within a temperature range of 80-100 °C. Mostly, the proposed working temperature of driveline components is 80 °C.

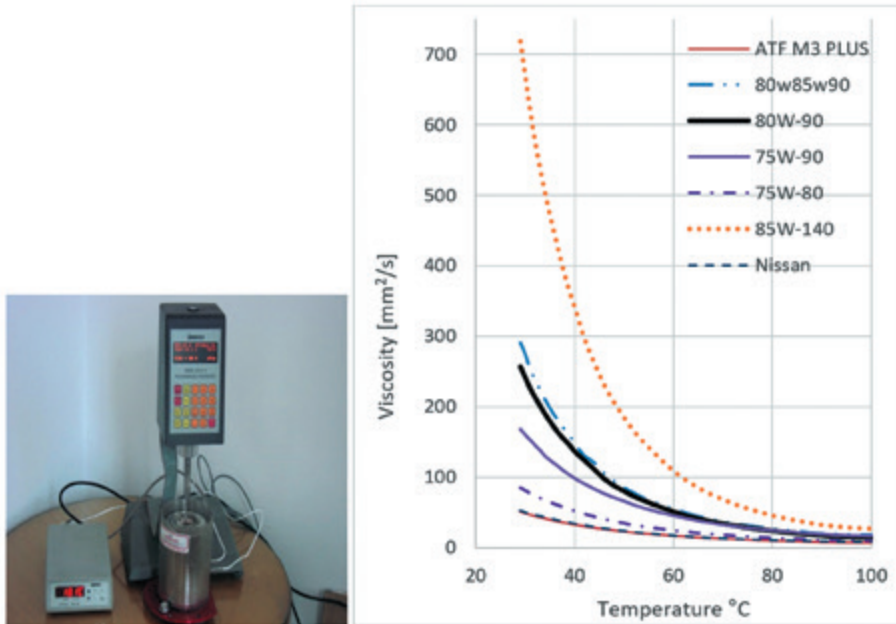


Fig. 5. Oil viscosity test station and example test results

The capabilities of the test rig presented will be exemplified by the examination of a prototype planetary gear unit with a basic (geometric) gear ratio of $i_o = 3.1372$ (Fig. 6), for both directions of power transmission, i.e. for the gear unit operating as a reducer and a multiplier.

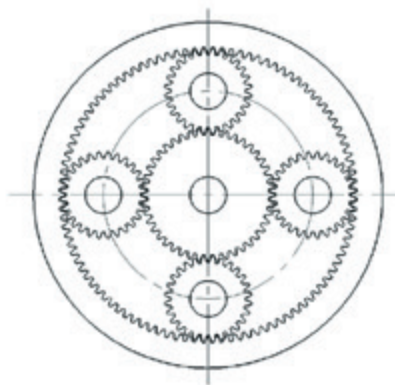


Fig. 6. Schematic diagram of a single planetary gearset with four planet gears and $i_o = 3.1372$

The basic variables measured during the tests were input and output shaft torques and rotational speeds, oil temperature, and gear housing vibrations.

The tests were performed with constant torque on the output shaft of the gear unit under test and with the rotational speed of the input shaft being stepwise changed from minimum to maximum and back to minimum (Fig. 7). For the measurements, T40B torque meters manufactured by HBM were used, whose maximum acceptable rotational speed was 20 000 rpm and maximum errors of measuring the torque and shaft rotation angle were $\pm 0.02\%$ and $\pm 0.05\%$, respectively. Thanks to the high accuracy class of these instruments, pulsations of the quantities measured on the shafts could be recorded and appropriate analyses could be carried out.

During the measurements, the oil temperature changed by as much as $10\text{ }^{\circ}\text{C}$, in spite of the use of an external oil cooling system with temperature stabilization. The oil grade was 80W-90 and its moisture and particulate matter contents measured during the tests were 15 % and 32 ppm, respectively.

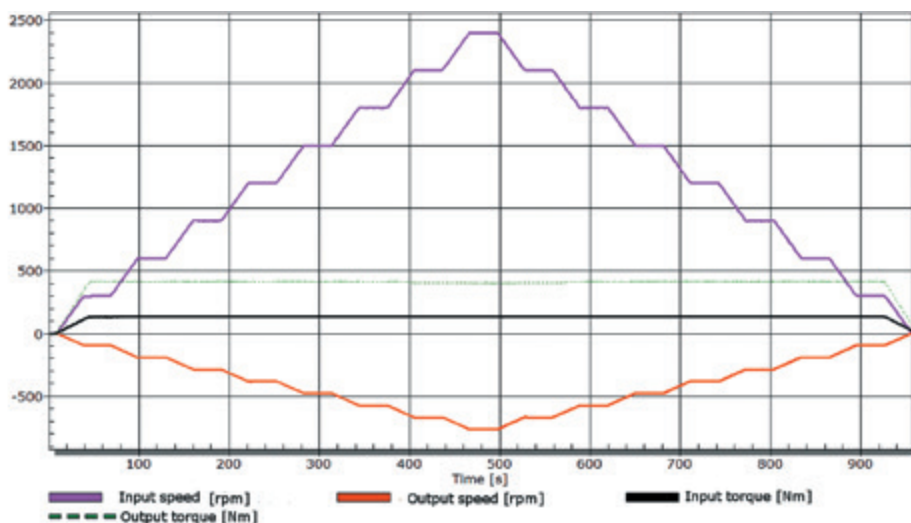


Fig. 7. Example readout of the parameters measured on the input and output shaft

2. Efficiency: Results of Measurements and Calculations

An example result of determining the efficiency of the planetary gear unit under test from direct measurements and of adjusting it to a uniform (constant) temperature of $80\text{ }^{\circ}\text{C}$ has been presented in Figs 8a and 8b, respectively.

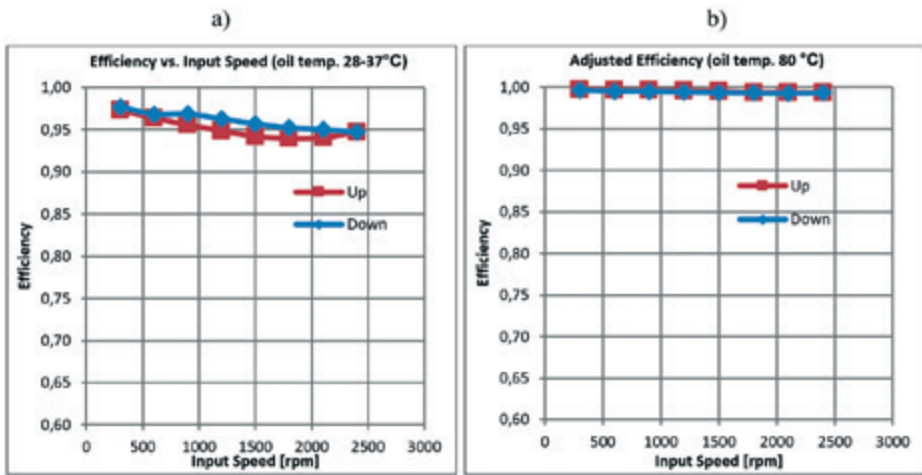


Fig. 8. Efficiency curves of the planetary gear unit operating as a reducer

The gear unit efficiency values determined from direct measurements were adjusted (reduced) to a uniform (constant) temperature (adopted here as an example level of 80 °C), according to the formula below, with taking into account the oil viscosity changes as presented in Fig. 5:

$$\eta_{80^{\circ}C} = 1 - \left(1 - \frac{M_{wy}}{M_{we} i_o} \right) \frac{\nu_{80^{\circ}C}}{\nu_{eksp}} \quad (1)$$

where: $\eta_{80^{\circ}C}$ – gear unit efficiency at an oil temperature of 80 °C;
 $\nu_{80^{\circ}C}$ – oil viscosity at a temperature of 80 °C;
 ν_{eksp} – oil viscosity at the actual experiment temperature;
 M_{wy} – output torque;
 M_{we} – input torque;
 i_o – kinematic ratio of the gear unit under test.

The gear unit efficiency determined without taking into account changes in the oil viscosity during measurements, i.e. changes in the churning loss, is defined by the formula:

$$\eta_{eksp} = \frac{M_{wy}}{M_{we} i_o} \quad (2)$$

The gear unit efficiencies as functions of torque, rotational speed, and oil temperature for the unit operating as a reducer and multiplier have been presented in Figs 9 and 10, respectively. The graphs show strong efficiency dependence on the oil temperature and wide ranges of gear unit operation with high efficiency. The surfaces corresponding to oil temperatures of 30 °C and 80 °C define the space of the efficiency values with which the

gear unit may operate. The differences between the efficiency values for the gear unit operating as a reducer and multiplier are small, within the limits of measurement error (Figs 11 and 12). In both gear unit operation modes, the efficiency increased with growing values of the torque transmitted; with rising speeds, the efficiency slightly declined. The test results were handled without any approximation procedure, which is evidenced by local sharp bends (edges) on the surfaces shown in the graphs.

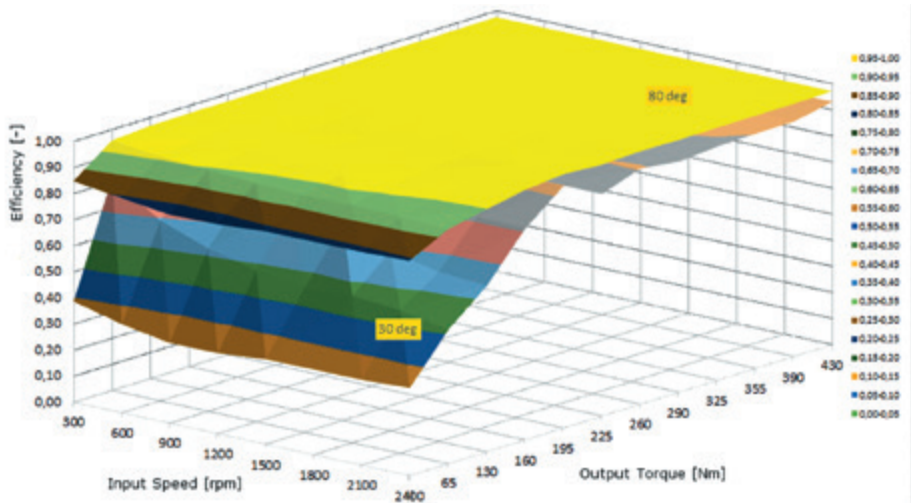


Fig. 9. Gear unit efficiency as a function of torque, rotational speed, and oil temperature (top surface for 80 °C and bottom surface for 30 °C) for the unit operating as a reducer

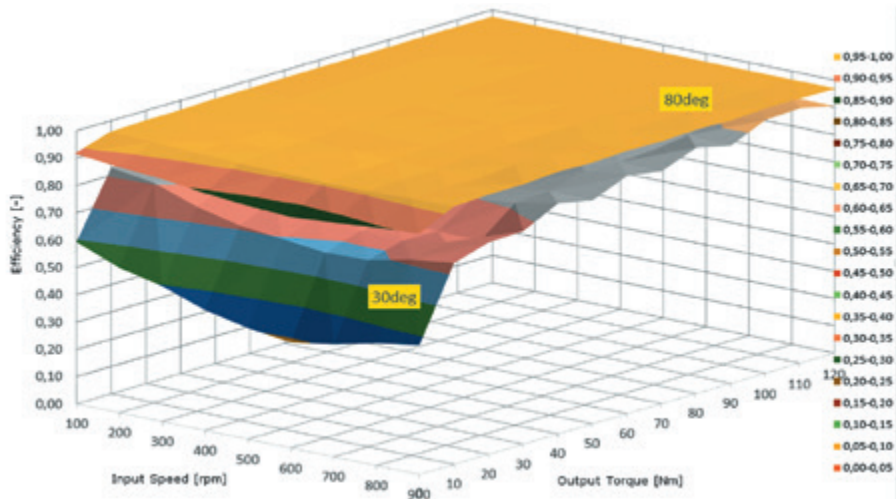


Fig. 10. Gear unit efficiency as a function of torque, rotational speed, and oil temperature (top surface for 80 °C and bottom surface for 30 °C) for the unit operating as a multiplier

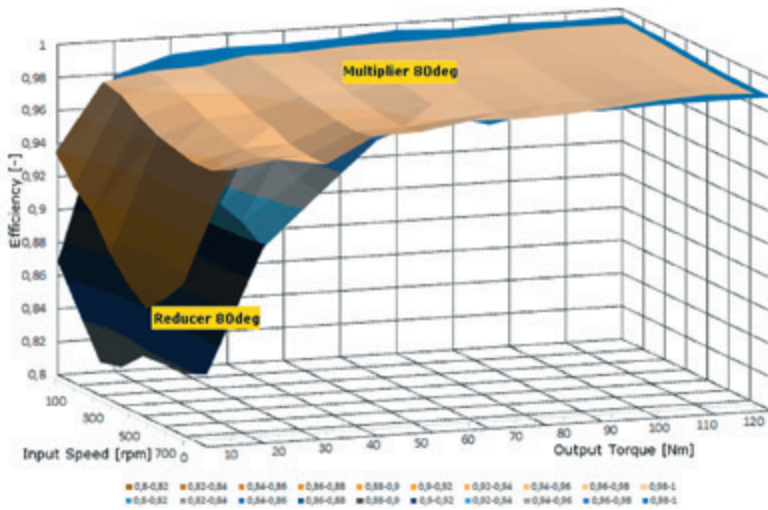


Fig. 11. Gear unit efficiency as a function of torque and rotational speed for both gear unit operation modes, at an oil temperature of 80 °C

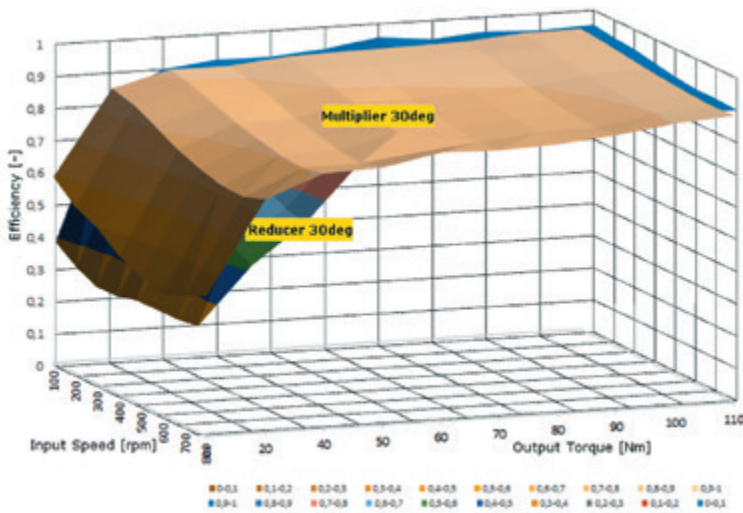


Fig. 12. Gear unit efficiency as a function of torque and rotational speed for both gear unit operation modes, at an oil temperature of 80 °C

Figs 13 and 14 show torque losses for different gear ratio values; the constant losses and churning losses as well as the oil temperature impact may be separately discerned (the upper curves correspond to lower oil temperatures for rising rotational speeds in the test cycle).

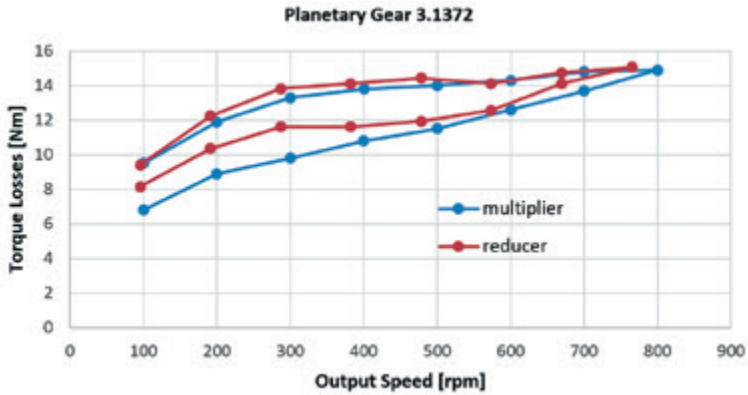


Fig. 13. Torque losses in the planetary gear unit, reduced to the output shaft

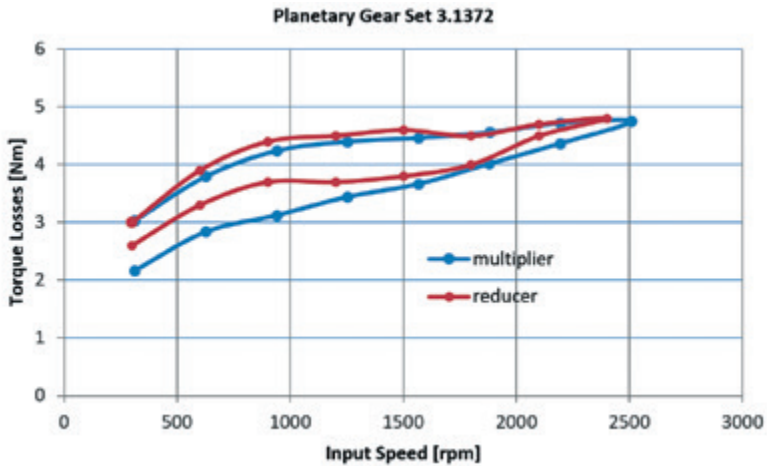


Fig. 14. Torque losses in the planetary gear unit, reduced to the input shaft

The efficiency of the planetary gear unit under test may be compared with the theoretical efficiency determined from the following formulas [1]:

Reducer
$$\eta_{h1} = \frac{i_o \eta_o - 1}{i_o - 1} = \frac{3.1372 \times 0.98 - 1}{3.1372 - 1} = 0.9706 \quad (3)$$

Multiplier
$$\eta_{h1} = \frac{i_o - 1}{\frac{i_o}{\eta_o} - 1} = \frac{3.1372 - 1}{\frac{3.1372}{0.98} - 1} = 0.9709 \quad (4)$$

The gear unit efficiency thus determined is constant in the whole range of loads and rotational speeds and is practically identical for both the reducer and multiplier unit operation modes. The rig test results confirmed these values, except for the range of low loads and for oil temperatures other than 80 °C.

3. Vibrations

In a planetary gear unit, there are many sources of vibrations caused by cyclic movement of the mesh zones in relation to the housing, including the varying gear mesh forces acting between the planets and the sun and ring gears. The frequencies of such vibrations depend on the kinematic layout of the gear unit and they are modulated by rotational speeds of the shafts.

In a planetary gearset, the basic vibration frequencies are [2]:

- mesh frequency f_m :

$$f_m = \frac{|n_1 - n_h|}{60} z_1 \quad (5)$$

- ring gear engagement frequency f_2 :

$$f_2 = \frac{|n_1 - n_h|}{60 |i_o|} s \quad (6)$$

(s – number of planets in the gearset under consideration)

- sun gear engagement frequency f_1 :

$$f_1 = \frac{|n_1 - n_h|}{60} s \quad (7)$$

- planet engagement frequency f_p :

$$f_p = \frac{|n_1 - n_h|}{60} \frac{z_1}{z_p} = \frac{|n_2 - n_h|}{60} \frac{|z_2|}{z_p} \quad (8)$$

- rotational frequency of the planet carrier f_{oh} :

$$f_{oh} = \frac{|n_h|}{60} \quad (9)$$

- rotational frequency of the output shaft f_{o1} :

$$f_{o1} = \frac{n_h (1 - i_o)}{60} \quad (10)$$

As it can be seen in the test rig photograph (Fig. 1), each stationary component unit of the test rig drive train is separately fixed to the test rig baseplate, which practically does not transmit vibrations to the adjacent units thanks to its large mass (about 6 000 kg). Hence, the sensor readings may be considered as adequately representing the vibrations generated within the gear unit under test.

3.1. Mesh Frequencies – Results of Calculations and Measurements of a 4-planet gearset

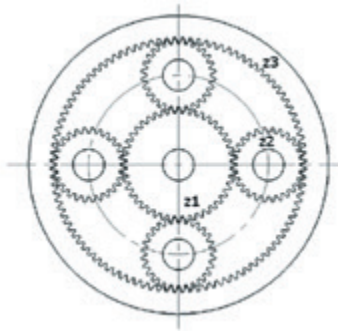


Fig. 15. A schematic showing the components of a 4-planet gearset

The gear unit under test was a planetary gearset (Fig. 15) with the following specifications:

1. Number of teeth of the sun gear $z_1 = 51$
2. Number of teeth of each of the planets $z_2 = 28$
3. Number of teeth of the ring gear $z_3 = 109$
4. Number of the planets $k = 4$
5. Kinematic ratio $i_o = 3.1372$

Calculations for the gearset operating as a reducer:

1. Input rotational speed = sun gear speed:

$$n_1 = 300; 600; 900; 1\ 200; 1\ 500; 1\ 800; 2\ 100; 2\ 400 \text{ rpm}$$

2. Planet carrier speed, absolute:

$$n_c = n_1 [z_1 / (z_1 + z_3)] = 95.6; 191.3; 286.9; 382.5; 478.1; 573.8; 669.4; 765 \text{ rpm}$$

3. Mesh frequency:

$$f_m = [z_1 z_3 / (z_1 + z_3)] (n_1 / 60) = 173.7; 347.4; 521.2; 694.9; 868.6; 1\ 042; 1\ 216; 1\ 390 \text{ Hz}$$

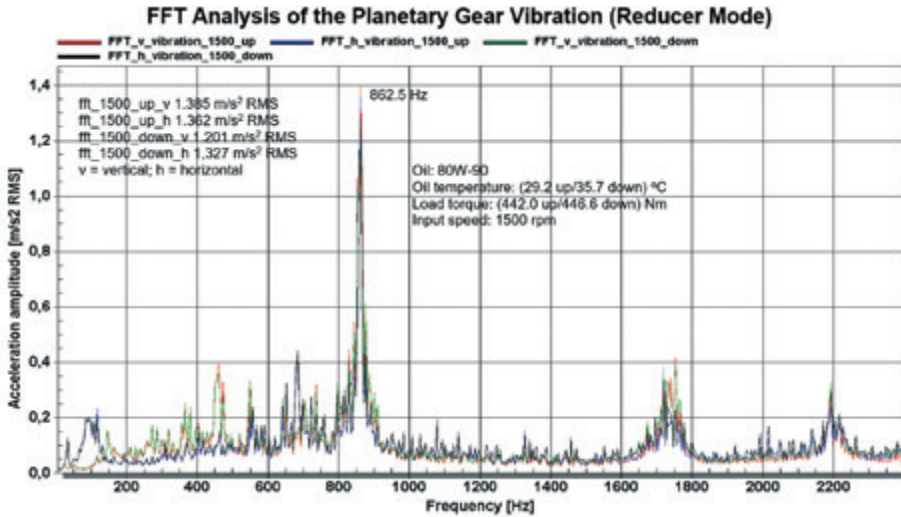


Fig. 16. Comparison of the FFT analysis results for vertical and horizontal vibrations

As it can be seen in Fig. 16, the FFT spectra coincide with each other, for both the vertical and horizontal vibrations and for both the increase ("up") and decrease ("down") in the rotational speed during the test cycle. No differentiation is observed, either, for changes in the load torque (Fig. 17), except for the loads that are close to the torque losses in the gear unit under test (Figs 18 and 19).

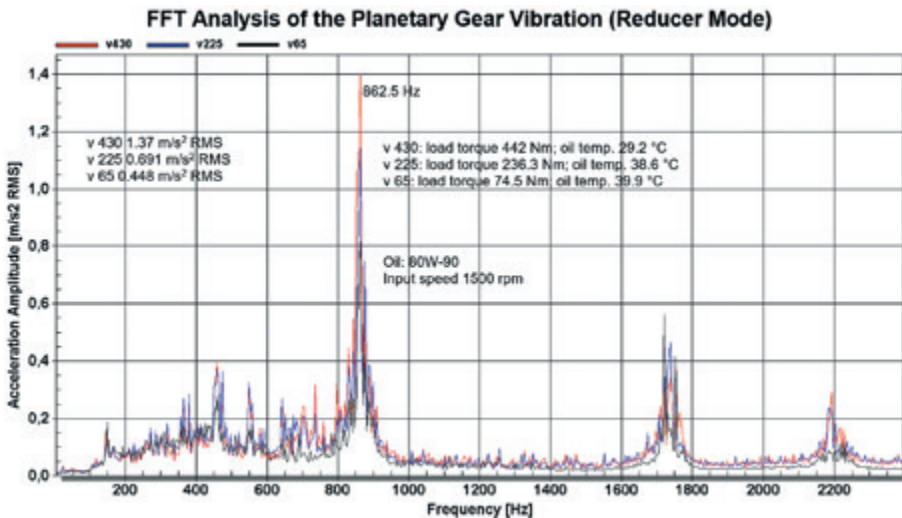


Fig. 17. FFT vibration analysis for various load torques

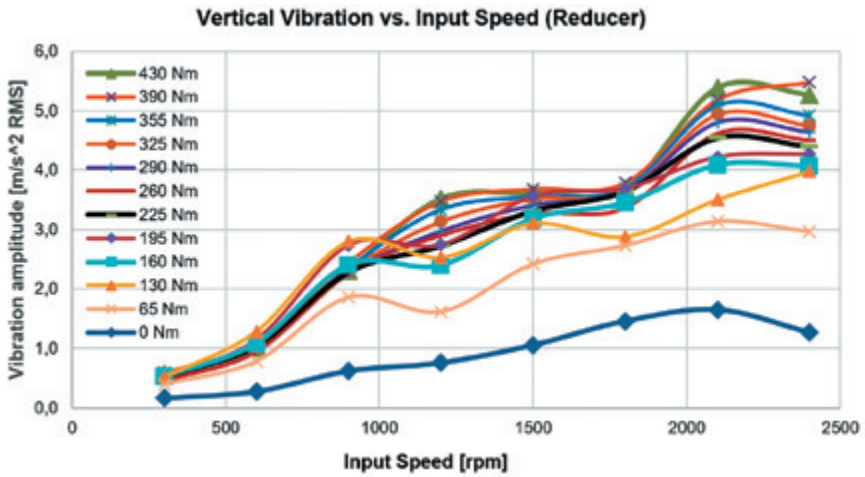


Fig. 18. Vertical vibrations as functions of rotational speed and load torque

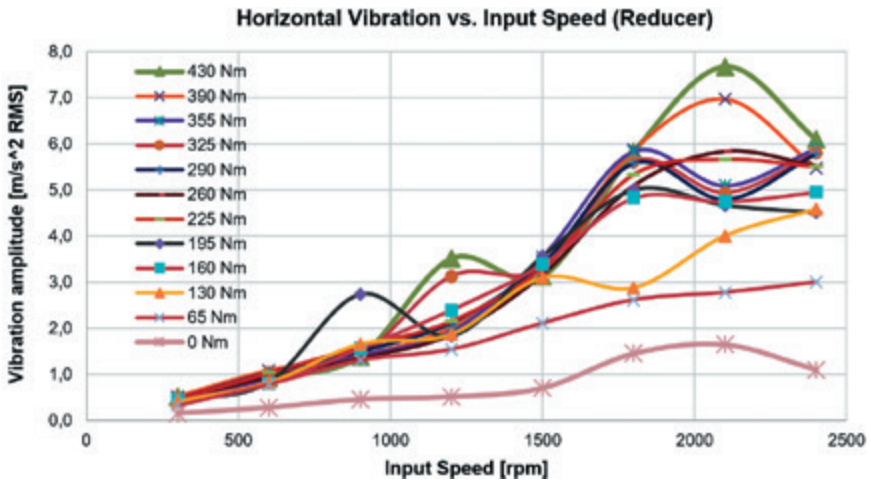


Fig. 19. Horizontal vibrations as functions of rotational speed and load torque

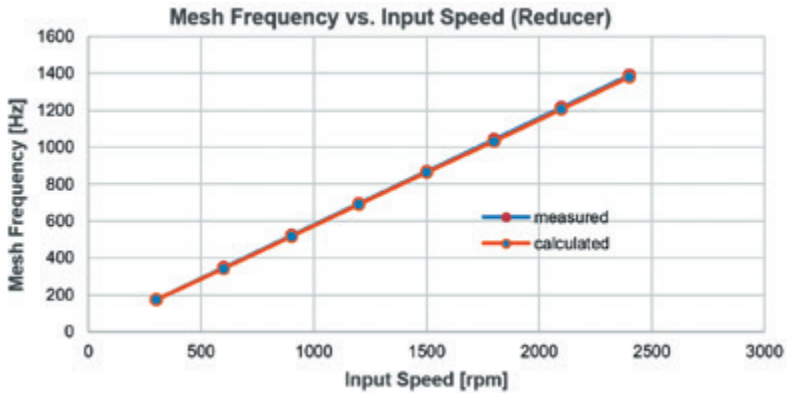


Fig. 20. Comparison of theoretical (calculated) and measured mesh frequency values

Table 1. Comparison of theoretical (calculated) and measured mesh frequency values (reducer mode)

Input speed [rpm]	Calculated mesh frequency [Hz]	Measured mesh frequency [Hz]
300	173.7	173.4
600	347.4	342.2
900	521.2	515.6
1 200	694.9	689.1
1 500	868.6	862.5
1 800	1 042	1 031
2 100	1 216	1 205
2 400	1 390	1 378

The characteristic frequencies depend on the gear unit input speeds (Figs 18, 19, and 20).

Calculations for the gearset operating as a multiplier:

1. Input rotational speed = planet carrier speed:

$$n_c = 100; 200; 300; 400; 500; 600; 670 \text{ rpm}$$

2. Sun gear speed, absolute:

$$n_1 = n_c [(z_1 + z_3) / z_1] = 313.7; 627.5; 941.2; 1255; 1569; 1882; 2096 \text{ rpm}$$

3. Mesh frequency:

$$f_m = z_3 (n_c / 60) = 181.7; 363.3; 545; 726.7; 908.3; 1 090; 1 212 \text{ Hz}$$

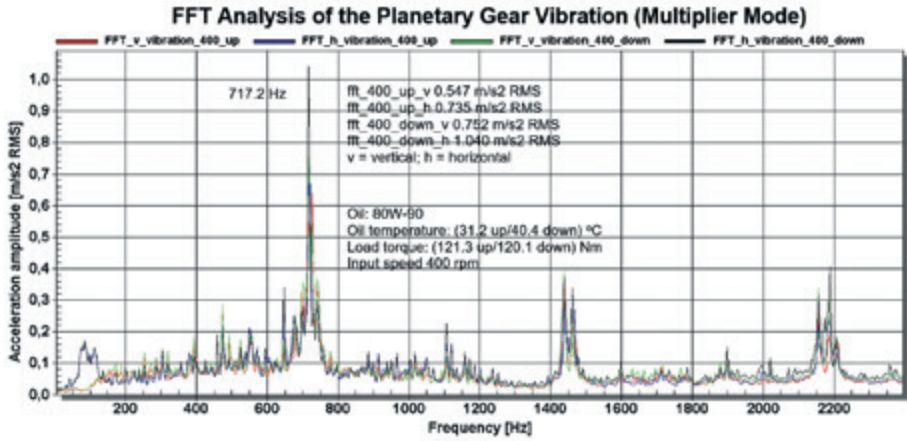


Fig. 21. Comparison of the FFT analysis results for vertical and horizontal vibrations

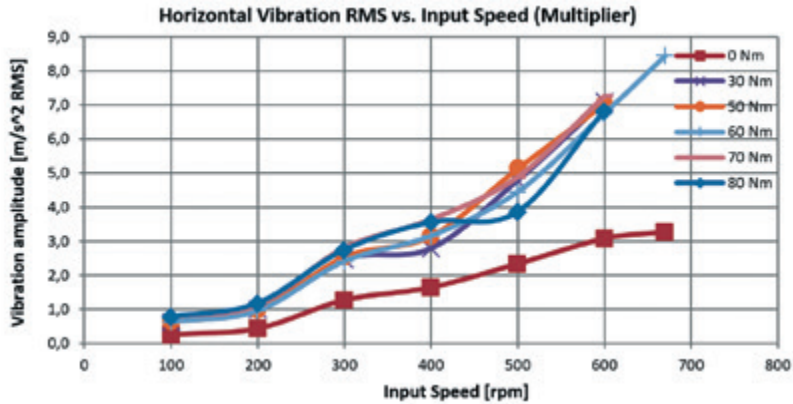


Fig. 22. Horizontal vibrations as functions of rotational speed and load torque

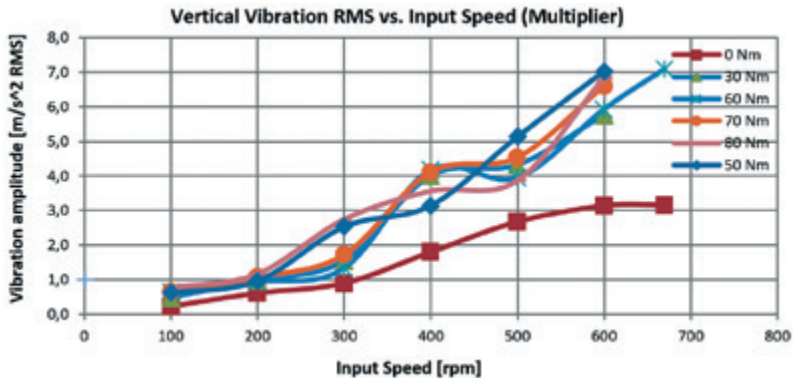


Fig. 23. Vertical vibrations as functions of rotational speed and load torque

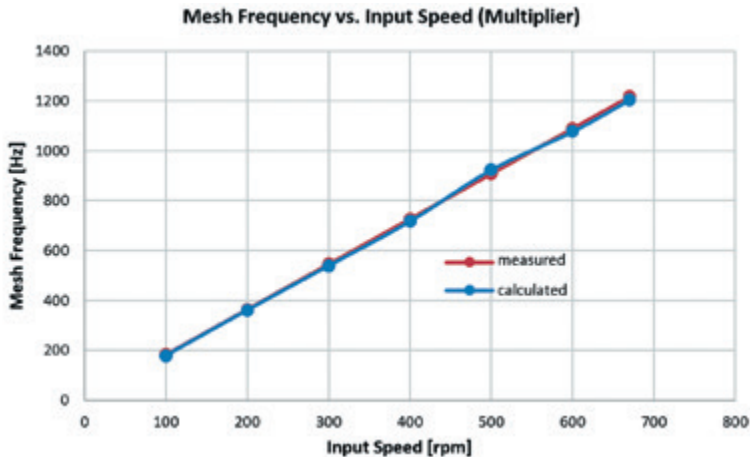


Fig. 24. Comparison of theoretical (calculated) and measured mesh frequency values

Table 2. Comparison of theoretical (calculated) and measured mesh frequency values (multiplier mode)

Input speed [rpm]	Calculated mesh frequency [Hz]	Measured mesh frequency [Hz]
100	181.6	182.8
200	363.3	360.9
300	545	539
400	726.7	721.9
500	908.3	923.4
600	1 090	1 078
670	1 217	1 210

The tables and graphs presented above show good consistency between the mesh frequency values determined theoretically (by calculations) and experimentally (by measurements), for both the reducer and multiplier mode of operation of the planetary gear unit.

When analysing the test results, it may be useful to introduce the following two parameters:

- dynamic gear ratio, defined as the ratio of the output torque to the input torque (Fig. 7):

$$i_M = \frac{M_2}{M_1} \quad (11)$$

- kinematic gear ratio, defined as the ratio of the rotational speed (angular velocity) of the output shaft to the one of the input shaft (Fig. 7):

$$i_k = \frac{n_1}{n_2} = \frac{\omega_1}{\omega_2} \quad (12)$$

The measured time histories of the gear ratios thus defined have been shown in Fig. 25.

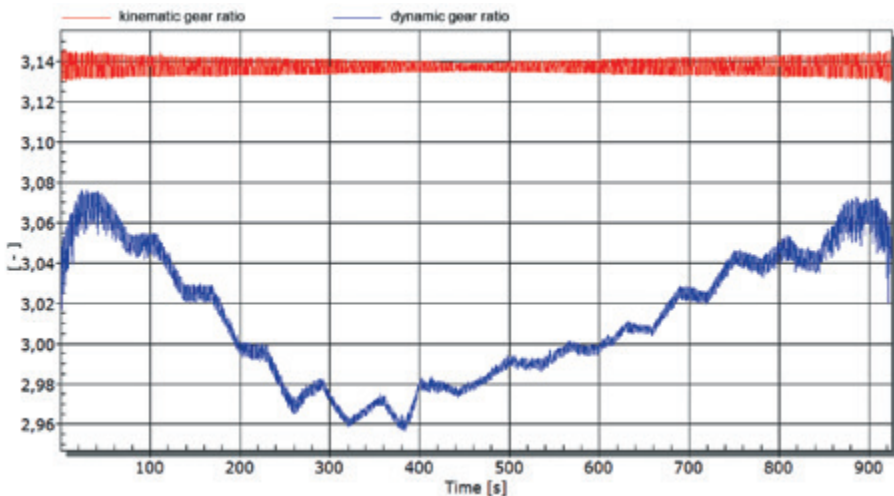


Fig. 25. Time histories of the kinematic and dynamic gear ratios during the test cycle

Based on an analysis of the gear ratio vs time curves, the following statements may be made:

- The dynamic gear ratio values significantly differ from the geometric (basic) gear ratio value $i_0 = 3.1372$. With a growth in the rotational speed, this difference increases, which translates into a decline in the gear unit efficiency.

- The amplitude of changes in the kinematic gear ratio i_k around the basic gear ratio value $i_o = 3.1372$ may be a measure of accuracy of the transmission of motion by the gear unit.
- The oscillations in the time histories of both gear ratios are the biggest for the lowest speeds and they decline with a growth in the speeds, which may suggest an increase in vibration damping in the gear mesh with rising centrifugal forces.
- The impact of changes in oil temperature (viscosity) during the test cycle was not taken into consideration.

4. Test rig noise

The noise emission measurements during the examination of the prototype planetary gear unit played only a subsidiary role. The A-weighted sound pressure levels were measured at a single measuring place in the vicinity of the gear unit under test. The K_{1A} and K_{2A} environmental correction factors (PN-EN ISO 11202) were not determined.

Results of noise measurements carried out on the test rig for the gear unit operating as a multiplier in specific conditions have been presented in Fig. 26. The measurement results obtained for the increase ("up") and decrease ("down") in the rotational speed during the test cycle practically did not differ from each other. The test rig noise increased with rising speeds of the gear unit, which corresponds well to growing RMS values of vibration amplitudes for higher speeds in the test cycle (Figs 22 and 23).

No difference in the test rig noise level was observed during the tests, whether the gear unit was examined in the reducer or multiplier operation mode.

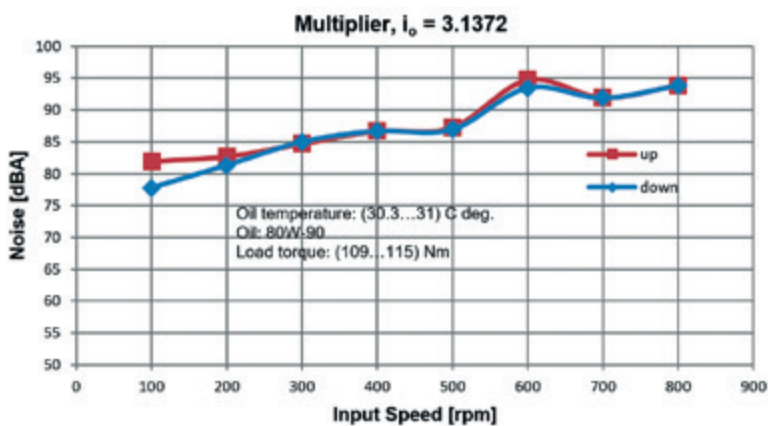


Fig. 26. Test rig noise level measured for the planetary gear unit operating as a multiplier

5. Conclusions

An analysis of the results of examining the prototype planetary gear unit on the test rig presented herein provided grounds for the following conclusions:

- The differences in the efficiency values determined for the gear unit operating in the reducer and multiplier modes were small, falling within the range of measurement errors.
- The gear unit efficiency depended on the torque transmitted, speed, and lube oil temperature (viscosity). The efficiency values increased with growing torque and slightly declined with growing speed.
- In the frequency spectrum, the vibrations with mesh frequency predominated. The vibrations determined by FFT analysis of the vibration signals measured were in good consistency with calculation results.
- The RMS values of vibration acceleration amplitudes increased with growing torque transmitted and input speed. Their characteristic curves indicated the presence of strongly damped resonance phenomena in the gear unit under test.
- The amplitude of changes in the kinematic gear ratio i_k around the basic gear ratio value $i_o = 3.1372$ may be a measure of accuracy of the transmission of motion by the gear unit.
- The dynamic gear ratio values significantly differed from the geometric (basic) gear ratio value $i_o = 3.1372$. With a growth in the rotational speed, this difference increased, which translates into a decline in the gear unit efficiency.
- No difference in the test rig noise level was observed for the tests with the gear unit examined in the reducer and multiplier operation mode.

The results presented herein are only a part of the data collected during the tests. They confirm that the test rig is suitable for multipurpose applications and, thanks to instrumentation with sensors of high accuracy class and to the software provided, enables comprehensive analyses of driveline components examined and diagnostic testing of their technical condition.

The full text of the article is available in Polish online on the website <http://archiwummotoryzacji.pl>.

Tekst artykułu w polskiej wersji językowej dostępny jest na stronie <http://archiwummotoryzacji.pl>.

6. References

- [1] Müller L. Przekładnie obiegowe (Epicyclic transmissions). PWN. Warszawa 1983.
- [2] Karray M, Chaari F, del Rincon A F, Viadero F, Haddar M. An Experimental Investigation of the Dynamic Behavior of Planetary Gear Set. Proceedings of the Fifth International Conference on Design and Modeling of Mechanical Systems. CMSM'2013 Djerba, Tunisia, March 25-27, 2013.
- [3] Wilk A, Łazarz B, Madej H. Wykorzystanie sygnału drganiowego korpusu do diagnozowania przekładni obiegowych (Using housing vibration signal in planetary gear diagnosis). Available from: www.obrum.gliwice.pl/upload/downloads/spg/100/09_Wilk.pdf.
- [4] Pawelski Z, Woźniak M. Badania stanowiskowe i symulacyjne przy wejściowym sygnale sinusoidalnym na wale turbiny przekładni hydrokinetycznej (Stationary and simulating researches with input sinus signal on turbine shaft of the hydrokinetic torque converter ZM130). Archiwum Motoryzacji. 2009; 2; 163-177.
- [5] Chao Huang, Jia-Xu Wang, Ke Xiao, Min Li, Jun-Yang Li. Dynamic characteristics analysis and experimental research on a new type planetary gear apparatus with small tooth number difference. Journal of Mechanical Science and Technology. 2013 (27); 5; 1233-1244.
- [6] Minghu Yin, Guoding Chen, Hua Su. Theoretical and experimental studies on dynamics of double-helical gear system supported by journal bearings. Advances in Mechanical Engineering. 2016 (8); 5; 1-13.
- [7] Gawande S H, Shaikh S N. Experimental Investigations of Noise Control in Planetary Gear Set by Phasing. Journal of Engineering. 2014 (2014), Article ID 857462, 11 pages.
- [8] Inalpolat M. A Theoretical and Experimental Investigation of Modulation Sidebands of Planetary Gear Sets. Dissertation. The Ohio State University. 2009.
- [9] Zhuang Li. Experimental Analyses of Vibration and Noise of Faulted Planetary Gearbox. Inter-noise. Melbourne, Australia, 16-19 November 2014.
- [10] Bartelmus W, Zimroz R. Metoda diagnostyki przekładni planetarnej (Planetary gearbox condition monitoring). Prace Naukowe Instytutu Górniczo-Politechniki Wrocławskiej. 2007; 118 (33).
- [11] Ericson T M, Parker R G. Experimental measurement of the effects of torque on the dynamic behavior and system parameters of planetary gears. Mechanism and Machine Theory. 2014 (74); 370-389.
- [12] Ericson T M, Parker R G. Planetary gear modal vibration experiments and correlation against lumped-parameter and finite element models. Journal of Sound and Vibration. 2013 (332); 2350-2375.
- [13] Hyun-Ku Lee, Koo-Tae Kang: An Experimental Study and Analysis on NVH Behaviors of the Planetary Gear Set. Journal of the Korean Society for Noise and Vibration Engineering. 2010 (20); 3; 242-248.